Integrated test programme for qualifying well cement slurries against formation gas intrusion

Skalle, P., Backe, K.R., Elvebakk, H., Justnes, H., Lile, O.B., Lyomov, S.K., and Sveen, J.

Norwegian University of Science and Technology

Presented at the
The international conference on development of off-shore oil and gas fields in Russia - The state of the art and perspectives
22-25 November, 1994, St. Petersburg, Russia.

INTEGRATED TESTING PROGRAMME FOR QUALIFYING WELL CEMENT SLURRIES AGAINST FORMATION GAS INTRUSION

by

Pål Skalle, SPE, **Knut R. Backe**, **Harald Elvebakk**, **Harald Justnes***, **Ole Bernt Lile**, SPE, **Shteryo K. Lyomov**, SPE, **Jostein Sveen***
NTH
Norwegian Institute of Technology
University of Trondheim
*SINTEF, Trondheim

Summary To investigate the ability of a cement slurry to resist the influx of formation gas under high pressure, several parameters that could characterize the cement were measured during the curing period from mixing to final set:

Permeability, tensile strength, external shrinkage, total shrinkage, hydrostatic pressure and electrical conductivity.

The most important parameters are permeability and tensile strength, determined through destructive tests at several time steps. In a special constructed cell electrical conductivity was measured continuously. In the same cell the cement slurry was exposed to gas with variable overpressure while subjected to a confining pressure. The gas flow into the cement was monitored. The behaviour of the parameters during the curing process have been utilized to characterize a cement slurry's resistance against formation gas intrusion.

INTRODUCTION

Well cement is used for cementing the steel casing to the wellbore and thus isolate the formation from the well. Sometimes gas from high pressure gas zones enters the annulus and makes its way through the cement. Gas intrusion probably occurs when the hydrostatic pressure of the cement slurry falls below the formation gas pressure. The main cause of the hydrostatic pressure decline is volume reduction of the slurry simultaneously with a gel strength development in the slurry which hinders downward flow to compensate for the volume loss. Fluid loss, temperature changes and elastic properties of the formation may also play an important role, but volume reduction alone is assumed to be able to account for the observed effect of pressure decline in the laboratory.

Various physical properties of and processes in the cement have been examined before and during the curing period:

- permeability
- tensile strength
- temperature
- electrical conductivity
- hydrostatic pressure
- self induced gas flow
- gas flow velocity
- shrinkage
- standard cement slurry control parameters

To compare the basic properties of gas tight slurries and gas leaking slurries, 6 HTHP gas tight cement slurries were formulated by three different cement service companies operating in the North Sea. Gas tight slurries were defined by Hibbeler et al.[1] as:

Low initial gel strength
< 10 lb/100 ft^2 YP
Fluid loss control
< 50 cc/30 min
Low free water
< 1%, 0% if inclined wells
Main transition
< 20 min. (40 - 70 Bc)
Staggared thicken.time
> 1 hour diff. betw. lead and tail slurry

(The latter characteristic doesn't apply to this work).

For comparison with the gas tight slurries 5 gas untight slurries were selected, characterized as simple, basic slurries with no gas tight properties as those stated above.

TEST PROCEDURES AND MEASURING PRINCIPLES

The test procedures and measuring principles applied in this study are all well known, although some of them were applied in a new manner. After receiving a sack of G-cement, the cement was packed in smaller air tight plastic sacks to avoid segregation and absorption of moisture. Additives were premixed dry or wet in destilled water. The slurries were mixed in 4 litre batches in a Waring Blender. Cement powder and dry additives were added to water in 15 s at 15 000 rpm and then stirred at 18 300 rpm for 55 s. The slurry was then characterized through the Bingham rheological model, by its free water content, density and consistency in accordance with API RP 10 B[2] and 13 B[3].

Temperature and hydrostatic pressure profile

Temperature is an indicator of the exothermic process. The start of an increase in temperature indicates the initiation of the hydration process (initial set). When the temperature culiminates, it indicates that the cement is hard (final set). The temperature and the hydrostatic pressure of the slurry were measured in a 30 cm high cylinder of ID 5 cm.

Permeability and tensile strength

In the beginning of the setting of the cement in the annulus, the porosity is high, between 50 and 65 %, depending on w/c ratio. Since the water essentially is a free fluid, the initial permeability is high. To quantify the potential for gas flow through the pore system as a Darcy flow, the permeability was measured at specific points of time during curing of the cement.

In order for gas to enter the cement, the differential pressure between the gas and the pore pressure either has to exceed the entry pressure of the capillary pressure curve or the strength of the cement matrix. The entry pressure and the form of the capillary pressure curve are controlled by the pore size distribution in the cement as shown in **fig. 1**. The capillary pressure, p_c, may be estimated by equ. (1):

$$p_c = \frac{2\,\sigma \cos\theta}{r}$$

in which, as typical example, the pore throat radius, r, is equal to 0.1 μm (10^{-7} m), surface tension, σ, between gas and solid surface is here set to $100 \cdot 10^{-3}$ N/m, while the wettability angle, θ, is set to 0 (non-wetting), resulting in an entry pressure of:

$$p_c = 2 \cdot 10^6 \text{ Pa (20 bar)}$$

The flow of gas through the pore system depends on the permeability of the flowing fluids. Since the pores primarily are waterfilled, the introduction of gas in the pores will start with pure fluid flow (displacement of water) and gradually turn the fluid flow into a two phase flow. To find the absolute permeabilities of gas and water in the two phase flow, the absolute permeabilities of gas and water measured in a monophase system have to be multiplied by the relative permeabilities for gas and water, respectively.

Fig. 2 shows the general curve shape of capillary pressure curves and relative permeability curves for water and gas. After first having overcome the entry pressure, the differential pressure and the form of the capillary pressure curve will then control how much gas will displace the water and thus decide the resulting gas saturation in the cement. If the gas is to move through the cement as a Darcy flow in a two phase system, the driving pressure gradient has to overcome the resistance against gas flow at that water saturation point. The permeability for gas at high water saturations is very low, as may be seen from the relative permeability curve.

It seems therefore reasonable to conclude that if formation gas is to intrude into and migrate through a normal well cement (with pore throat size reducing additives), it probably has to fracture the cement matrix and move through micro fractures. To create a hydraulic fracture, an excess gas pressure above the minimum strength of the cement slurry, i.e. the tensile strength, is necessary.

During permeability tests on cement slurries, Plee et al.[4] observed a sudden increase in hydraulic water loss during a continuos increase of the differential pressure. This behaviour was only seen after the induction period (2-3 hours after mixing) and was probably associated with the surpassing of a threshold stress causing a rupture of the brittle interparticular bonds generated by the hydration of calcium/aluminium silicates.

Cement slurries which are in a state between a liquid and a solid material, are not suited for being tested by ordinary solid strength parameters. However, measurement of the tensile strength by hydraulic fracturing the curing cement, probably results in a parameter closely tied to both gas intrusion and gas migration in the annulus.

An apparatus was constructed especially for the purpose of measuring both permeability and hydraulic fracturing strength. The apparatus and measuring procedure are presented in detail by Lile et al.[5]. A cell is filled with cement slurry into which water is pumped through a thin tube and a filter tip while the pressure is monitored, firstly at low rate to measure the permeability and then at high rate to measure the hydraulic fracturing pressure.

Shrinkage

Both total chemical and external chemical shrinkage have been measured. Total shrinkage was determined in a waterfilled bottle containing a 1 cm layer of cement, by measuring the amount of water that was sucked into the cement and the amount of water replacing the external shrinkage. External shrinkage was quantified by filling cement in a small flexible rubber sack, placing it under water and measuring the volume change indirectly by buoyance. So far, measurements have not been carried out at high temperatures. For a more detailed description we refer to Justnes et al.[6].

Electrical conductivity and gas flow monitoring

Because of chemical reactions within the slurry, the ion concentration of the pore water and the porosity

of the cement are changing during the curing process. By continuously measuring the electrical conductivity, it is possible to obtain an image of the reactions within the slurry.

In a cylinder shaped cell two end electrodes were used for current injection while the voltage drop was measured between two other electrodes. **Fig. 3** shows the realisation that was used. The cell consisted of several modules, each 7 cm long with an inner diameter of 5 cm. One of the modules was constructed with a section of steel tube insulated internally by a rubber sleeve and with teflon rings connecting it to the other modules. This design also allowed the use of confining pressure to avoid microannulus due to cement shrinkage.

The end plates of the cell were used as current electrodes using alternating current of 25Hz. This geometry gave a uniform electrical field. The potential difference was measured between electrodes situated in the teflon rings. The electrical conductivity, σ, may then be calculated through equation 2:

$$\sigma = (L/A)*(I/\Delta V) \qquad (2)$$

By monitoring the potential difference, ΔV, and the currency, I, between two electrodes, a distance L apart during the curing process, a continuos conductivity profile was obtained.

Simulation of gas migration

In order to simulate gas intrusion and migration and thereby being able to characterize the ability of a specific cement slurry to withstand gas migration, the apparatus shown in **Fig. 4** was developed. It is equipped with gas flow lines and valves for inlet and outlet, pressure regulators, gas flow meter and pressure transducers. Depending on the preset pressure condition, two main tests were performed:

1) self induced gas flow
2) forced/provoked gas influx

Self induced gas flow

The preset gas pressure, p_{gas}, in the inlet line, was adjusted at a level between the hydrostatic cement slurry pressure , p_{cem}, and the water gradient:

$$p_{cem} > p_{gas} > p_{H_2O} \qquad (3)$$

During the curing process, the cement would loose its hydraulic property and the hydrostatic cement pressure dropped. At a specific stage of the hydration process the gas pressure exceeded the cement pressure. At this condition gas entered the cement if the differential pressure overcame the entry pressure of the capillary pressure curve or the strength of the cement matrix. Gas intrusion in this way we termed self induced gas flow.

Forced gas influx

In order to compare slurries that are gas tight during self induced gas flow tests, gas flow was provoked by applying differential pressures high enough to force gas into the cement. The gas pressure in the inlet line at the chosen point of time was adjusted so that:

$$p_{gas} > p_{cem} \qquad (4)$$

If the amount of gas intrusion was large enough, the conductivity measurements indicated when the gas passed the electrodes by a drop in conductivity and thus monitored the gas migration upwards in the cement column. The gas migration velocity may thus be calculated.

RESULTS

Slurry control parameters

Table 1 presents all measured control parameters of the cements that were tested. In most cases the parameters were the average result of 2-4 repetitive measurements. Free water and rheology were notably different for basic slurries (denoted T) and gas tight slurries.

Temperature and pressure profile

Temperature and hydrostatic pressure profiles were measured for all slurries. In **Fig. 5** the curves are shown for the basic slurry T60. Initial set is not easily seen as the start of temperature increase after external heating, while final set is reached as the temperature culminates. The pressure, however, starts to drop immediately after initial set is reached. At this point gas may intrude the cement slurry.

A typical difference between basic slurries and gas tight slurries, was found in the hydrostatic pressure behaviour during the first 15 minutes or so of curing. A drop towards the hydrostatic pressure of water was only observed for low T basic slurries, caused by settling due to high free water content and low rheological properties of the cement.

Permeability and tensile strength

In **Fig. 5** tensile strength tests are presented for the T60 slurry. The test results are reproducible. The same is true for the permeability, although the data are more spread. In **Figs. 6** and **7** permeability and tensile strength for the A140 and B180 slurries are presented. All plots in these three figures are based on the average of 2-4 repetitive tests.

Shrinkage behaviour

In **Fig. 8** the external shrinkage for a T 60 slurry is presented as percentage of the initial volume. The volume reduction is quite rapid the first 10 hours after which it levels off. The total chemical

shrinkage, including also internal shrinkage pores, shows the same behaviour, but is twice as high and continues after the external shrinkage levels off.

Electrical conductivity

In **Fig. 9** the conductivity profile is plotted for the T60 slurry. The shape of the conductivity curves is characteristic and repetitive for all 5 electrodes. This indicates a high degree of reliability of such measurements. The main shape of the conductivity curves is controlled by the temperature and the porosity of the cement. The temperature effect may be eliminated by using an approximate method[7]. The characteristic peaks on the curves image the hydration process: the preinduction period is seen after 1 hour (formation of OH^- and $H_3SiO_4^-$ ions) and the induction-acceleration period after 5-6 hours (super saturation of Ca^{2+} ions). The culmination of the main curve at 3.5 hours, indicating a decrease in porosity, shows the start of the hydration reaction (initial set).

Self induced gas flow

Self induced gas flow was obtained when the hydrostatic cement pressure dropped below the constant gas pressure. Initial gas pressure was 3.75 bars while hydrostatic slurry pressure was 3.9 bars. At 4 hours the differential pressure, p_{gas}-p_{cem}, became positive and gas started to flow. The flow rate was only 0.3 ml/min. (normalized to 0°C and 1 atm.), which was too low to be indicated by the electrical conductivity measurements. Self induced gas was only obtained in the low T basic slurries.

Gas flow velocity

To test the response of gas flow through the slurry on electrical conductivity, gas was forced into the cement by increasing the gas pressure. **Fig. 10** shows two tests where the differential pressure was increased at 1 hour and 3 hours after mixing of the cement. The gas flow rate increases instantaneously and shortly after the first electrode pair exhibits a sharp decrease in conductivity. The indications by the other four pairs of electrodes follow almost linearly as a function of time. Before gas reaches the column between the electrodes, there is a small characteristic increase of the conductivity, supposedly caused by the displaced filtrate front.

DISCUSSION

The temperature is the most important parameter for tracking the onset of the initial and the final set. However, it does not give information about the ability of the cement to withstand gas intrusion and migration.

For this purpose, other parameters are better indicators. A systematic interpretation of the relationship between all measured parameters, for all basic slurries and all the gas tight slurries revealed that the key difference between the two types of cements may be seen in the hydrostatic pressure and the tensile strength behaviour. For the untight cements, the pressure fell almost immediately down to the water column pressure, stayed constant for some time and continued thereafter to fall. The gas tight pastes maintained the hydrostatic cement pressure until a very sharp decline at a specific point in the hydration process. Build-up of tensile strength was generally also much faster for the tight than for the untight cements. Hence, the critical period was much shorter and the possibility for gas influx lower. The permeability dropped rapidly to very low values in both cement types as the hydration starts, faster for the tight cements, though. The same was true for the conductivity where it fell very rapidly to a low level for the tight cement types, whereas the untight cements showed a gradual decrease.

All these parameters have been included in a common gas tightness factor, more thoroughly discussed by Lile et al[5]. They have tested the reliability of this factor by comparing with results from actual leak tests, either the test cell of **fig. 3** or a larger test all. The Gas Tightness factor, abbreviated as the GT-factor, finally got the form:

$$GT = \sqrt{\Delta t} \cdot \frac{k_1 - k_2}{k_1} \cdot k_2 \left(\frac{p_H - p_1}{p_H} + 1 \right)$$

Δt is the time window for the tensile strength to start increasing (at time t_1) and reach a specific value (at time t_2). At time t_2 the cement is hard. Δt should be as small as possible. k_1 and k_2 are the permeability at the two points of time, t_1 and t_2. The permeability should be as low as possible within the time window. The hydrostatic pressure at time t_1 is p_1 while p_H is the hydrostatic pressure of the fresh cement slurry. The decrease in hydrostatic pressure should be as small as possible before the strength starts building up, in order to resist gas migration caused by high formation pressure.

From the above considerations the best slurry to resist gas migration should be the one with the lowest GT-factor. Tests so far[5] have indicated that slurries with GT-factor >5 are leaking.

CONCLUSIONS

Known measuring principles have successfully been applied to characterize cement slurry properties during the hydration process. Permeability and tensile strength were measured by means of darcy flow and hydraulic fracturing, respectively, using water. Both properties are repetitive and measurable until final set. Shrinkage properties of cement were recorded in a simple and reliable manner, but measurements are so

far limited to 60°C. Hydrostatic slurry pressure, gas flow and electrical conductivity were monitored in an 80 cm high laboratory cell, consisting of several modules. The chemical curing process have been monitored by electrical conductivity, which is a function of ion concentration in the cement pore water and the porosity. The cell was used to run self induced and forced (provoked) gas influx tests, and, when sufficient gas was flowing, the gas front could be tracked by the electrical conductivity measurements.

The correlation between the measured parameters have been summarized in a gas tightness-factor, the GT-factor, which has been proven reliable for this purpose.

ACKNOWLEDGEMENT

The authors would like to extend their thanks to the sponsors of this work: the Royal Norwegian Council for Scientific and Industrial Research (NTNF), Norsk Hydro as, Saga Petroleum as and Statoil as, and their representatives Svein Joakimsen, Øystein Kalvenes, Jan Erik Olvin and Nils Ivar Nødland for their personal engagement and contributions.

REFERENCES

1. Hibbeler, J.C., DiLullo, G. and Thay, M,: "Cost-effective gas control: A case study of surfactant cement", paper SPE 25 328 presented at the SPE Asia Pacific Oil & Gas Conference, Singapore (Feb. 8-19, 1993)
2. API RP 10B: "Testing oil-well cements and cement additives", API, Dallas, Texas, 1978.
3. API RP 13B: "Standard Procedure for testing drilling fluids", API, Washington, 1982.
4. Plee, D., Lebedenko, F., Obrecht, F,. Letellier, M and van Damme, H.: "Microstructure, permeability and rheology of bentonite-cement slurries", Cem. and Concrete Research, Vol. 20, No 1 (1990) 45-61
5. Lile, O.B., Skalle, P., Elvebakk, H., Backe K.R., and Lyomov, S.K.: "A new technique for measuring permeability and strength of a curing cement". NTH, U. of Trondheim. (1994). Submitted for publication.
6. Justnes, H., van Loo, D., Reyniers, B., Skalle, P., Sveen, J., and Sellevold, E.J.: "Chemical shrinkage of oil well cement slurries," NTH, U. of Trondheim. (1994). To be published.
7. Schlumberger Log Interpretation Charts 1989. Schlumberger Well Services.

Table 1. Control parameters for all slurries. Slurries denoted T are basic slurries, those denoted A through H are gas tight slurries, designed by different service companies.

Slurry no.	BHST	SG	t_{set} (h:min) to reach			FW	PV	YP
	°C		30, 40 and 70 Bc			ml	cP	lbs/100 ft^2
T30	30	1.89	2:30	3:12	2:40	3.5	52	110
T60	60	1.87	2:56	3:15	3:30	9.5	32	125
T90	90	1.86	3:00	3:17	3:25	8.5	62	96
T140	140	2.04				2.0	20	28
T180	180	2.13				1.0	15	20
C140	140	7.05	5:53	5:58	6:01	0		3.5
E140	140	2.05	2:29	2:30	2:33	0	90.0	15.0
A140	140	7.05	3:58	4:08	4:09	0		3.0
G140	140	2.05	2:40	3:12	3:18	<0.1	31.6	7.5
D180	180	7.15	4:49	4:50	4:51			3.0
F180	180	7.15	3:02	3:17	3:58	0	58.5	11.5
B180	180	2.15	3:23	3:24	3:25	0		2.25
B180	180	2.15				0		2.25
H180	180	2.15	5:25	5:26	5:26	<0.1	43.2	10.9

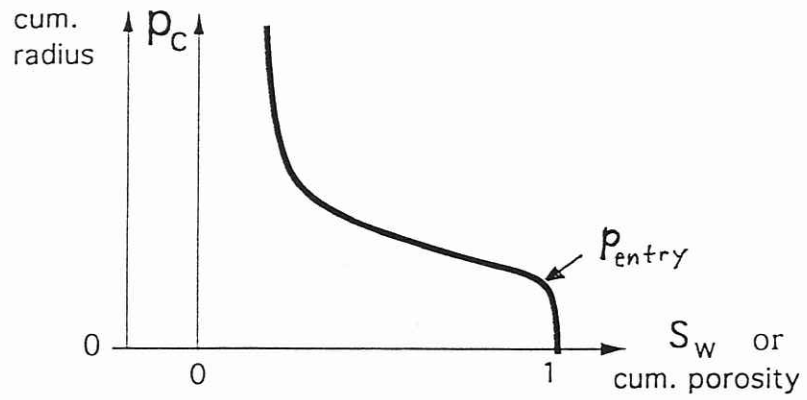

Fig. 1. The dependency between entry pressure and pore throat size distribution.

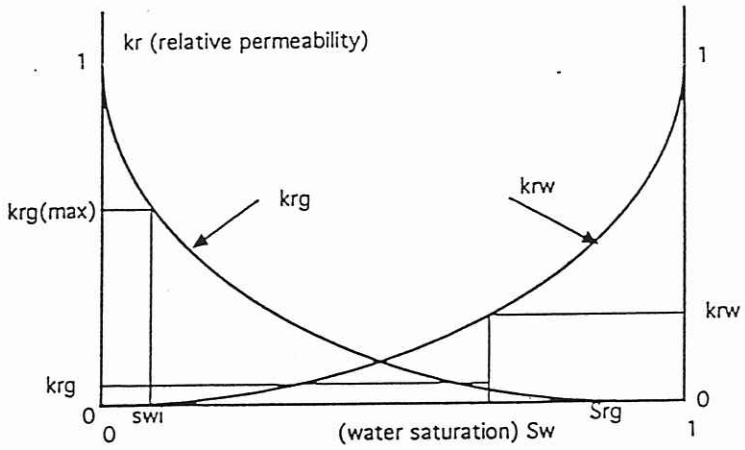

Fig. 2. General shape of capillary pressure and relative permeability curves.

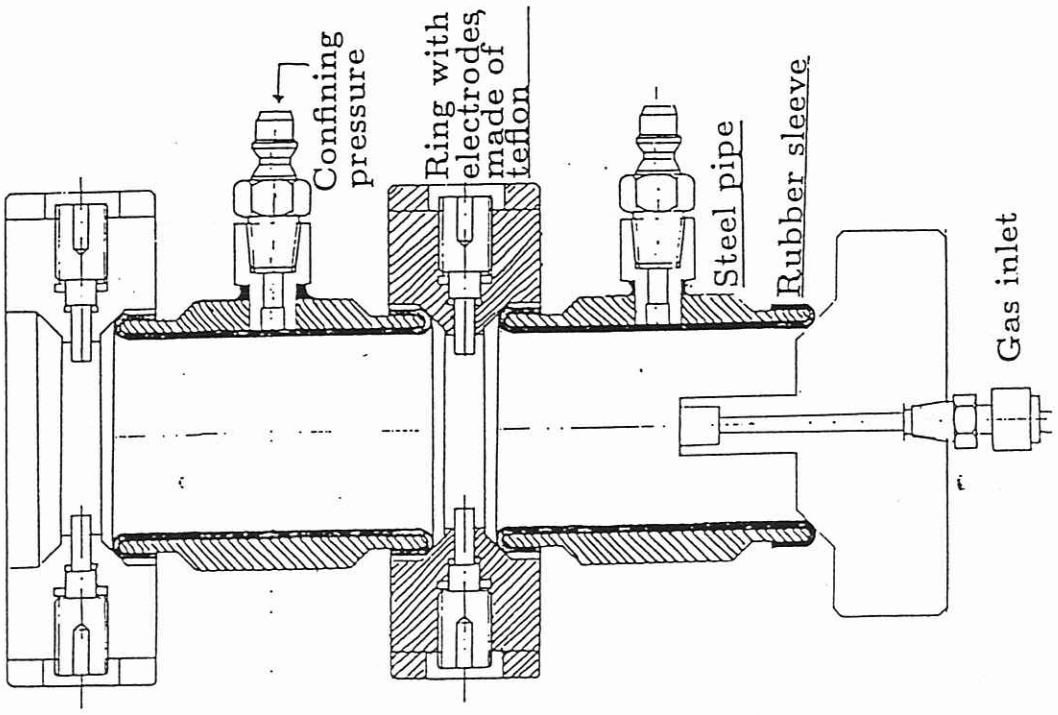

Fig. 3. Bottom module and first standard module of the test cell for cement slurries.

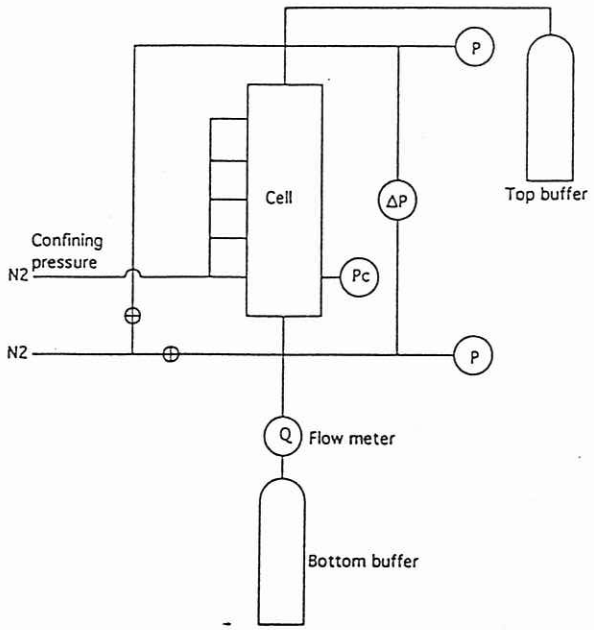

Fig. 4. Control flow chart of the cement slurry cell.

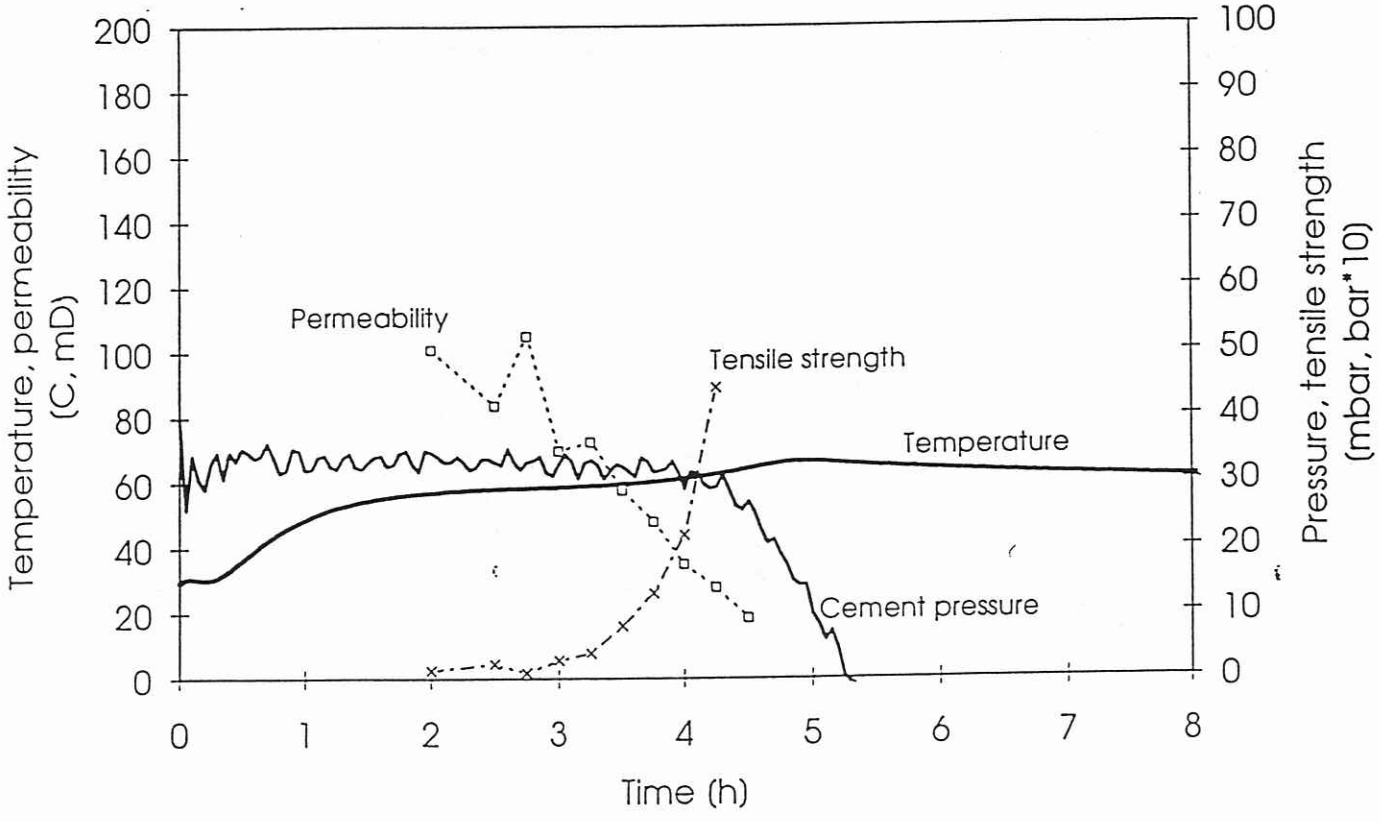

Fig. 5. Temperature, pressure profile, tensile strength and permeability development for the basic slurry T60.

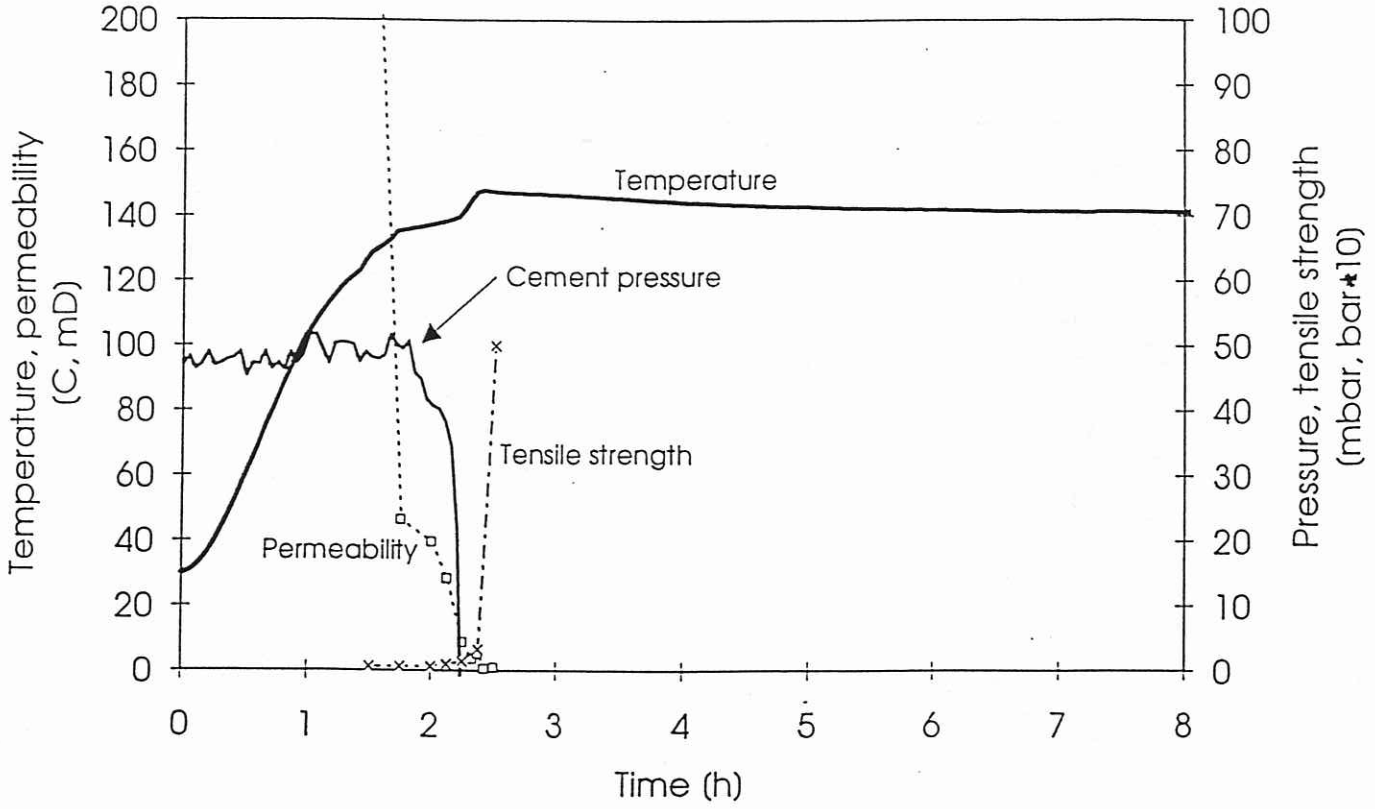

Fig. 6. Tensile strength and permeability development for the A140 slurry.

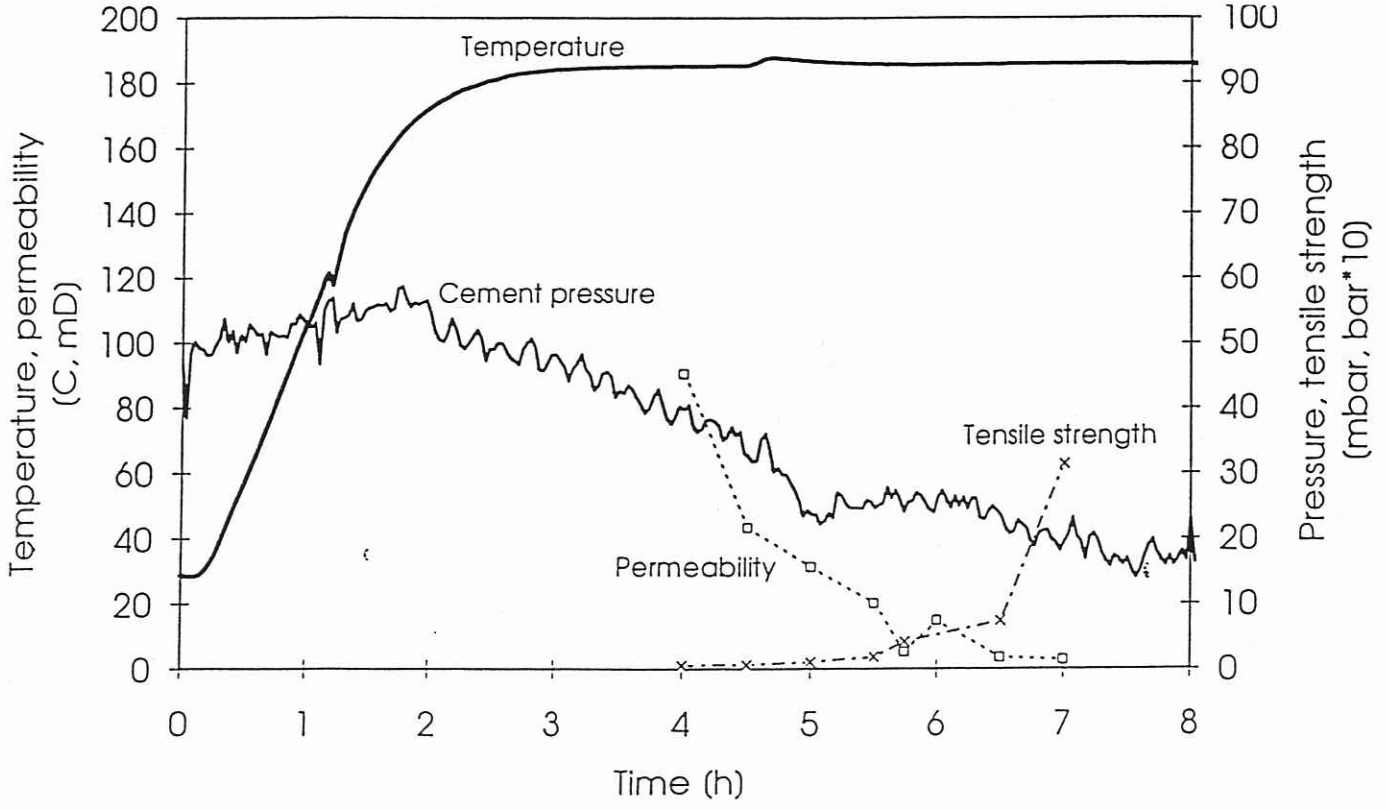

Fig. 7. Tensile strength and permeability development for the B180 slurry.

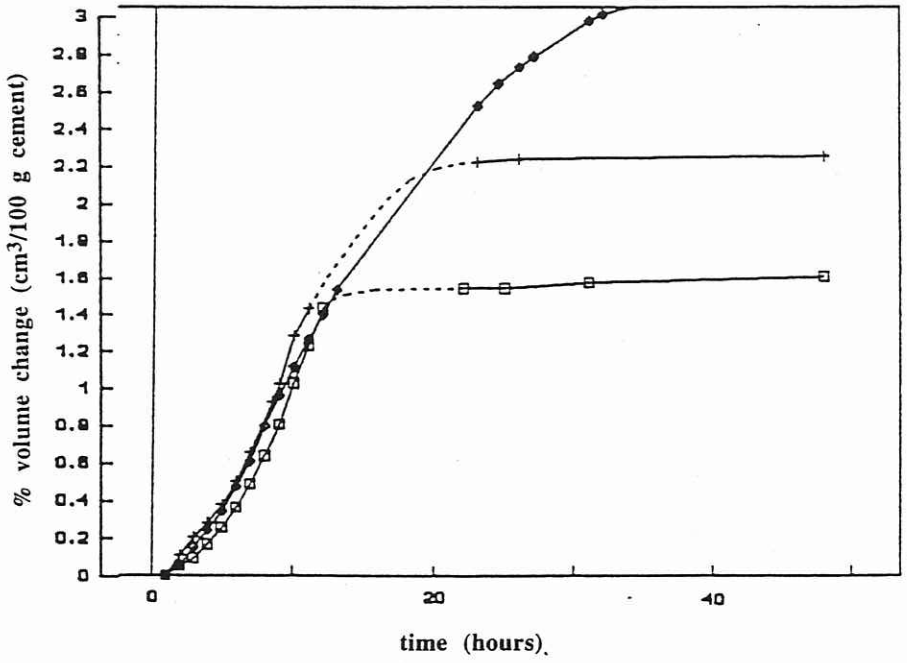

Fig. 8. External shrinkage for a T 60°C slurry.

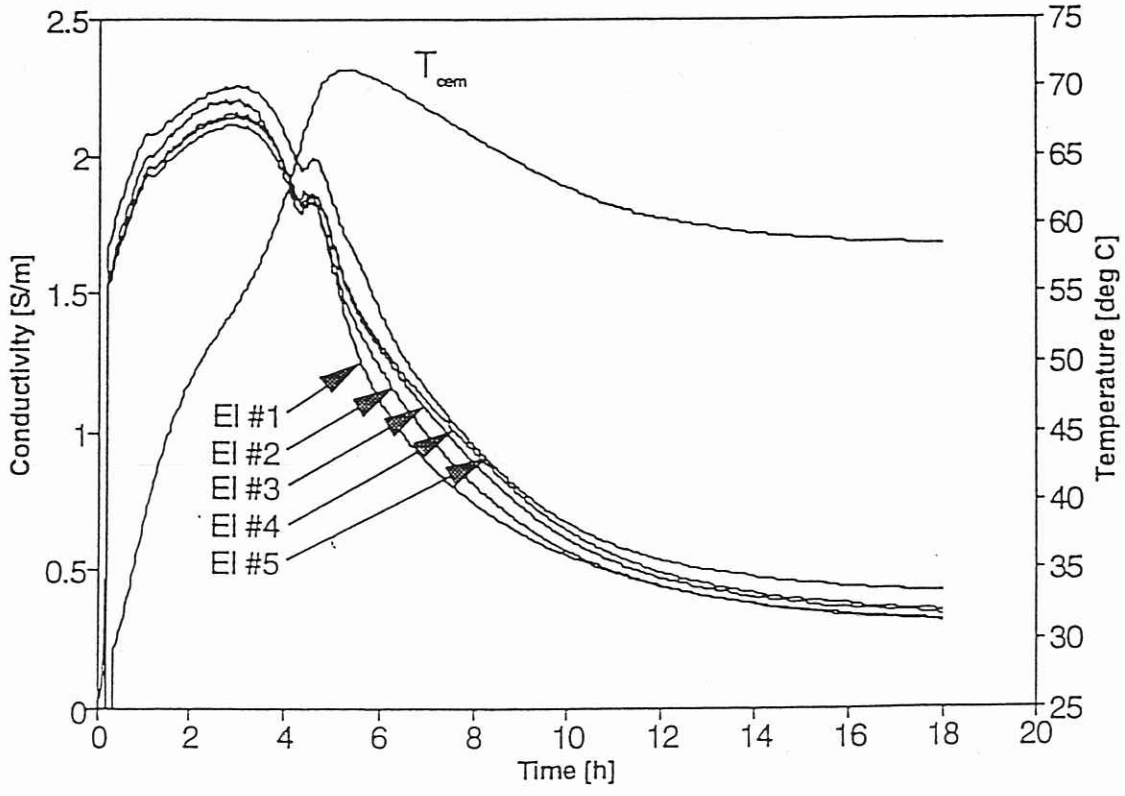

Fig. 9. Electrical conductivity during hydration in the T60 slurry. Not temperature corrected.

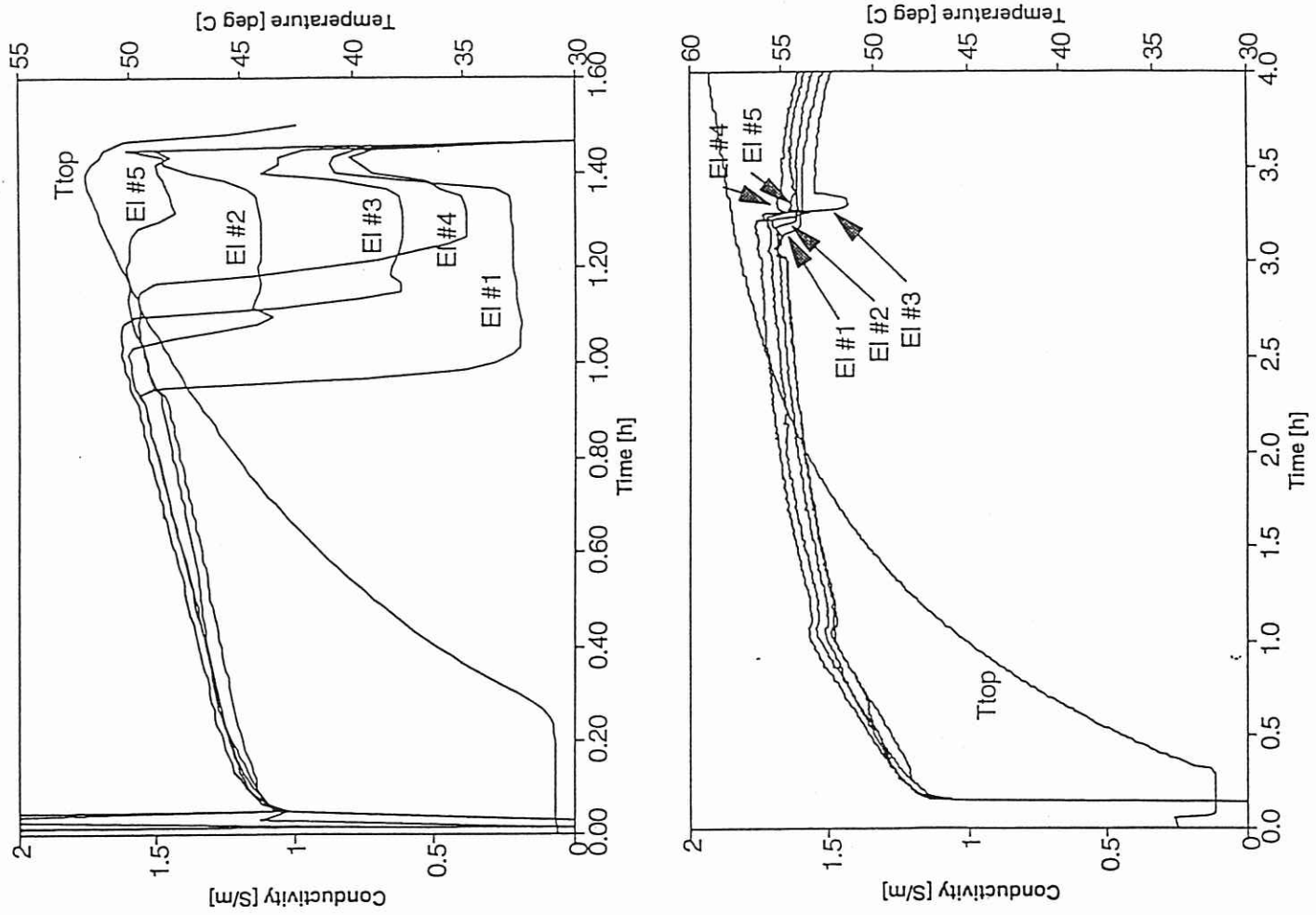

Fig. 10. Forced gas influx into the T60 slurry at 1 hour (upper figure) and 3 hours (lower figure) after mixing.

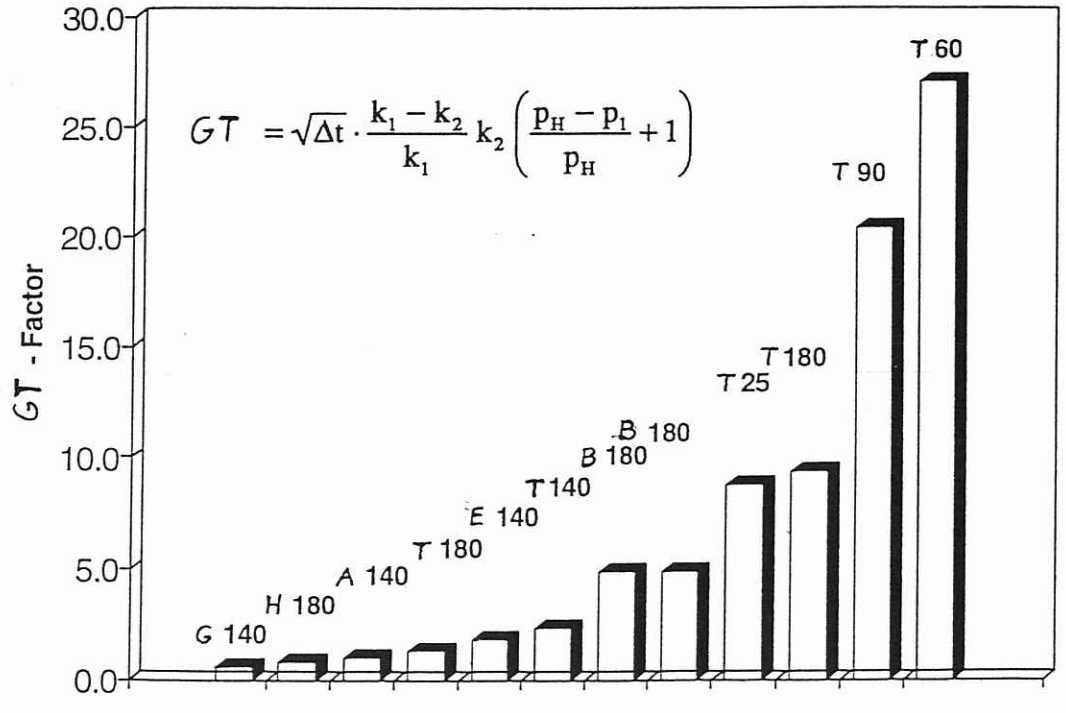

Fig. 11. Gas tightness factor for different gas tight slurries (A throuth H) and basic, gas untight slurries (T).